Available online at www.sciencedirect.com

ScienceDirect

Procedia CIRP 132 (2025) 68–73

www.elsevier.com/locate/procedia

12th CIRP Global Web Conference (CIRPe 2024)

Static stiffness analysis of an electronically preloaded rack and pinion feed drive system

Oier Franco [a*], Xavier Beudaert [a], Ibai Ulacia [b], Kaan Erkorkmaz [c], Jokin Munoa [a, d]

[a] *IDEKO, Dynamics and Control Department, Elgoibar, Basque Country, Spain*
[b] *Mondragon Unibertsitatea, Loramendi 4, Mondragon, Spain*
[c] *University of Waterloo, Precision Controls Laboratory (PCL), Waterloo, ON, Canada*
[d] *Mechanical Engineering Department, University of the Basque Country (UPV-EHU), Bilbao, Spain*

* Corresponding author. *E-mail address:* ofranco@ideko.es

Abstract

Rack and pinion feed drives are commonly selected for large machine tools with long travel distances due to their consistent stiffness, which remains unaffected by axis stroke. To mitigate the inherent backlash between the pinion and the rack, a double pinion setup with electronic preload, managed via CNC is typically used. This commissioned preload value not only influences the acceleration capacity, but also the stiffness behaviour of the feed drive system as demonstrated in this study. A coupled master-slave controlled rack and double pinion model is developed and validated through static stiffness measurements on a large-scale machine tool at varying levels of electronic preload.

Keywords: Machine tool feed drives; Master-slave control; Double rack and pinion.

1. Introduction

Modern machine tools are sophisticated mechatronic systems where the feed drive system plays a crucial role in positioning components carrying the tool and workpiece, determining part quantity and manufacturing productivity. Depending on operational needs, manufacturers may choose between ball screw, linear motor or double pinion and rack systems [1, 2]. Travel distance is a significant factor affecting both cost and performance. Ball screw drives are preferred for distances up to 4-5 meters due to their precise positioning and good efficiency-to-cost ratio [3]. In contrast, linear motors, which eliminate backlash and wear due to the absence of mechanical transmission elements, are more costly and used selectively where their benefits outweigh their expenses. For travels exceeding 5 meters, double pinion and rack systems are ideal as they maintain stiffness irrespective of distance. Uriarte et al. have recommended these systems for large machines requiring long travels and high load capacity [4].

Machine tools demand minimal backlash for accuracy. While powertrain systems are engineered to minimize clearance, the application of preload can further enhance precision. Preload force significantly impacts feed motion quality, dynamic behaviour, service life and energy consumption. Unlike direct drives with linear motors, which inherently have zero backlash and require no preload [1], ball screw and rack and pinion systems need a tensioning force to eliminate clearance.

In ball screw applications, the nut is preloaded to remove axial clearance between the recirculating balls and the screw's guiding slots, increasing contact stiffness. Temperature variations can alter this preload value [5, 6]. The most common method involves adjusting a spacer between two nuts, with the spacer's thickness determining the preload force [7]. Clearance can also be reduced by using slightly larger recirculating balls, but this is only feasible for small preloads due to increased wear from sliding contact. Excessive preload results in high wear and heat, so preload force is typically limited to 12% of dynamic load capacity, with a usual value around 6-8% [3]. Verl et al. proposed a design principle that reduces preload to enhance operational characteristics [8]. Direct preload identification is complex and rare in practice; however, the preload of an assembled ball screw can be measured by evaluating drag torque at 100 rpm with no external loads, as per

10.1016/j.procir.2025.01.012

DIN ISO 3408-3 [9]. Verl et al. discovered that pretension varies with feed velocity, being negligible at low speeds but significant at high speeds [10]. Zhou et al. analyzed the differences between traditional preload estimates and experimental values, developing a preload-adjustable ball screw to study the relationship between preload force and drag torque. Their new modeling approach improved prediction accuracy across three preload levels [11].

In double pinion and rack feed drives, backlash is the distance a gear moves along the pitch line before engaging a fixed gear. Backlash provides running clearance, accommodates manufacturing tolerances and reduces heat, noise, wear, and overload risks, thereby preventing drive failure [12]. In literature, two approaches aim to reduce clearance by applying preload. Mechanical solutions, such as split pinions [13], mechanical assemblies [14], and hydraulic actuation [15], are proposed but may not fully eliminate play between gear segments [16]. Commercially available single-motor gearboxes are cost-effective but lack adjustable preload without mechanical modifications [17]. In large machine tools with high torque requirements, drive parallelization enhances input torque and a secondary drive for pretension torque can mitigate nonlinear vibrations from backlash and axis feedback control [18]. The industry trend favors double motor actuation with electronic preload control via CNC controllers, simplifying drive design while increasing controller complexity, but nowadays CNC manufacturers provide this control solution. To perform electronic preload, the velocity control loop in double pinion and rack drives uses a master-slave coupling (Fig. 1.a). The master drive controls position and velocity, while the slave drive follows velocity setpoints from the master's position control loop [19], though recent approaches use data from both motor encoders [20]. Engelberth et al. reviewed control structures for preload induction [19]. Higher preload reduces maximum acceleration, but HEIDENHAIN's Motion-dependent Adaptation of Control parameters adjusts tensioning torque to enhance acceleration [21]. Verl et al. developed adaptive preload controls to increase energy efficiency [22], and Franco et al. [23] experimentally show the tool centre point dynamics variation for different preload values. Preload tuning lacks a clear guideline; Zirn suggests 10-30% of motor rated torque, while industrial standards favor 20-25% [18, 21]. Verl et al. found that a 4% preload adequately compensated for clearance [22]. This study examines how electronic preload affects static stiffness in a three-degree-of-freedom model validated with experimental data derived from a heavy-duty machine tool.

2. Feed drive model definition

Fig. 1.a shows the double pinion and rack feed drive model presented in this paper. The CNC generated trajectory (x_{ref}) is controlled by the proportional position control gain (K_{v}) which uses the driven load position, typically acquired by a linear encoder (x_{load}). The velocity reference ($\dot{x}_{\mathrm{ref}}$) is controlled by the master-slave configuration where each motor has a proportional-integral (PI) controller utilizing the rotational velocity of each motor via rotary encoders ($\dot{\varphi}_{\mathrm{m}}$ and $\dot{\varphi}_{\mathrm{s}}$). The desired preload level can be modified by adjusting a parameter called torque bias or tension torque (τ_{p}), defined as a percentage of the motor's rated torque. The torque equalization controller (PI_{preload}) generates additional speed setpoints for each motor, considering the desired torque preload. This control configuration allows the use of motors with different power ratings, providing individual weighting factors to adapt torque distribution (K_{Tm} and K_{Ts}). If both motors are identical, the load is shared proportionally by setting $K_{\mathrm{Tm}} = K_{\mathrm{Ts}} = 0.5$. The generated torque commands for master and slave are denoted as τ_{m} and τ_{s}, respectively. Additionally, external disturbance forces (F_{load}) can be directly applied to the load.

Power transmission requires low speed and high torque, necessitating additional gear steps. Planetary gearboxes, with multiple teeth engagement, increase torsional stiffness [24]. Thus, each motor's equivalent inertia can be computed via Eq. 1, where motor, gearbox and pinion inertias are jointly considered. The reduction factor (i_{red}) of the gearbox must also be considered in this calculation.

$$J_{\mathrm{eq}} = \left(J_{\mathrm{motor}} + J_{\mathrm{gearbox}}\right) + \frac{J_{\mathrm{pinion}}}{i_{\mathrm{red}}^2} \tag{1}$$

The stiffness of this feed drive mechanism is dominated by the torsional stiffness of the motor coupling (k_{coupling}), installed gearbox (k_{gearbox}), shaft (k_{shaft}) as well as the contact stiffness of the pinion and rack combination ($k_{\mathrm{p-r}}$) (Eq. 2, Fig. 1.b). In the proposed model, each motor is coupled to the load by a series of spring elements (i.e. k_{m}), which simplifies the intricate nonlinear behaviour of tooth mesh stiffness [25] by representing it as a constant value.

$$\frac{1}{k_{\mathrm{m}}} = \frac{1}{k_{\mathrm{coupling}}} + \frac{1}{k_{\mathrm{gearbox}}} + \frac{1}{k_{\mathrm{shaft}}} + \frac{1}{k_{\mathrm{p-r}}} \tag{2}$$

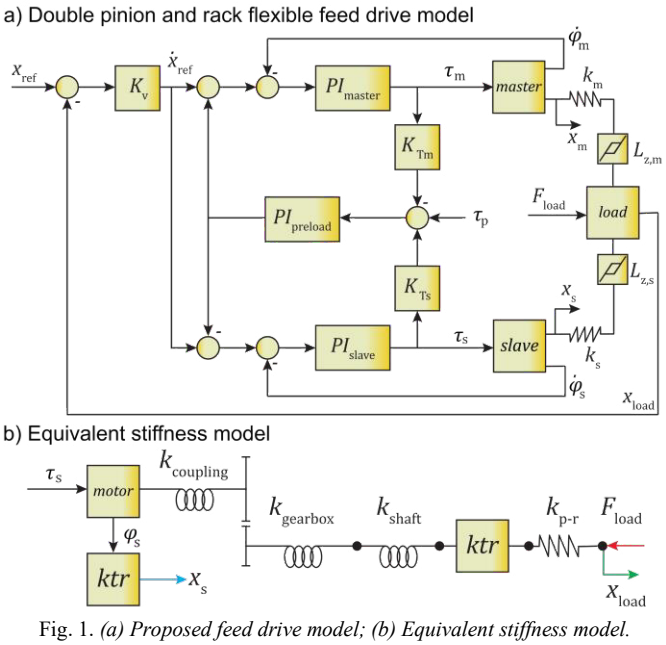

Fig. 1. *(a) Proposed feed drive model; (b) Equivalent stiffness model.*

The equivalent backlash in the power transmission path can arise from various sources, including motor-gearbox and pinion-rack joint interfaces, as well as accumulated clearances within the gearbox. This mechanical nonlinear behavior has been modeled using a dead zone approach [26]. $L_{\mathrm{z,m}}$ and $L_{\mathrm{z,s}}$ are the equivalent backlash values, between load and motor positions (i.e. x_{load} and x_{s}).

As a result of a commanded trajectory (x_{ref}), a reference torque (τ_{ref}) is generated to achieve the desired displacement. For standstill case, $\tau_{\mathrm{ref}} = 0$ Nm, the net torque (τ_{net}) which is the sum of each motor's torque, must be zero; otherwise, the machine will move (Eq. 3). Due to electronic preload, each motor at standstill generates the desired preload torque level τ_{p}. Within the interval $-2\tau_{\mathrm{p}} < \tau_{\mathrm{ref}} < 2\tau_{\mathrm{p}}$, both master and slave torque (τ_{m} and τ_{s}) have opposite polarities, meaning both pinions are on opposite flanks of the rack (Fig. 2 zone ②). A reference torque outside this interval induces a flank change in one of the pinions, depending on the direction of movement. Therefore, in such cases, the torques of each motor have the same polarity. Eq. 4 indicates the maximum net torque ($\tau_{\mathrm{net,max}}$) that can be obtained under preload conditions. Increasing the preload torque leads to a reduction in achievable acceleration. The inertias of the model have been obtained from suppliers' catalogues and the pinion inertia has been neglected. The inertia of the axis-driven load has been obtained from the machine CAD drawing. The next section presents the identification of the equivalent joint stiffness for each motor as well as the equivalent backlash.

$\tau_{\mathrm{net}} = \tau_{\mathrm{m}} + \tau_{\mathrm{s}}$, where

$$\tau_{\mathrm{m}} = \frac{\tau_{\mathrm{ref}}}{2} + \tau_{\mathrm{p}} \qquad (3)$$

$$\tau_{\mathrm{s}} = \frac{\tau_{\mathrm{ref}}}{2} - \tau_{\mathrm{p}}$$

$$\tau_{\mathrm{net,max}} = 2\left(\tau_{\mathrm{m,max}} - \tau_{\mathrm{p}}\right) \qquad (4)$$

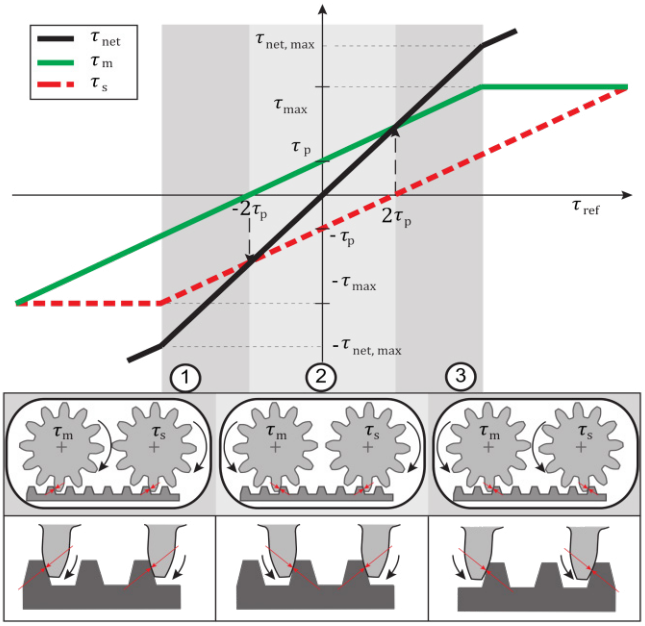

Fig. 2. *Electronic preload for backlash suppression.*

3. Experimental identification

To independently characterize each motor, the coupling between the master and slave motors must be removed. This involves modifying machine tool configuration parameters to close velocity and position loops with the encoder of the desired motor while disabling the other motor. The linear scale continues to monitor the load position for further analysis.

3.1. Joint equivalent stiffness

To perform a static stiffness analysis, the machine tool has been positioned at the initial travel distance. The force F_{load} has been generated by imposing a stepped position trajectory through a CNC command while limiting the displacement against the mechanical rigid bumper (Fig. 3). A Kistler 9212 load cell has been placed between the carriage and the bumper, acquired by dSPACE MicroLabBox. The maximum experimental commanded displacement has been chosen to obtain a force level of around 10kN, which corresponds to approximately 300 µm for this tested machine (Fig. 3). The displacements is acquired by the internal sensors through a dedicated software provided by the CNC manufacturer. As a result of the applied F_{load}, the generated deformation between the motor rotary encoder ($x_{\mathrm{m,s}}$) and load displacement acquired by the linear encoder (x_{load}) can be computed. An equivalent linear stiffness can be obtained, which considers all the transmission components within the force path (Eq. 2). The identification is done individually one motor at a time, by breaking the master-slave coupling. Fig. 4.b shows the fitted equivalent stiffness on top of experimental results obtained from the test shown in Fig. 4.a, resulting in different values for each motor: k_{m} = 81 N/µm and k_{s} = 100 N/µm.

3.2. Joint backlash

To identify the existing equivalent backlash, the master-slave coupling must be removed, operating each motor separately. No force load is applied, and a 1 mm back-and-forth movement is commanded. Fig. 4.c shows the position difference between each motor rotary encoder and load displacement ($x_{\mathrm{m,s}}$ and x_{load}). Here, the identified equivalent backlash combines all sources of backlash within the transmission. While the contribution of each element is complex, the gearbox backlash can typically be estimated as 0.04 of the tooth module [27]. The identified equivalent backlash for the master and slave motors are 314 and 363 µm respectively.

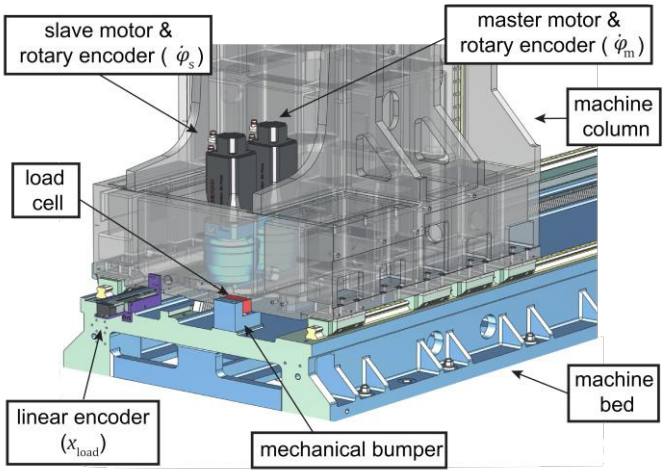

Fig. 3. *Machine tool component description.*

Using the experimentally determined stiffness and backlash, the electronically preloaded rack and pinion feed drive model shown in Fig. 1.a is validated in the next section.

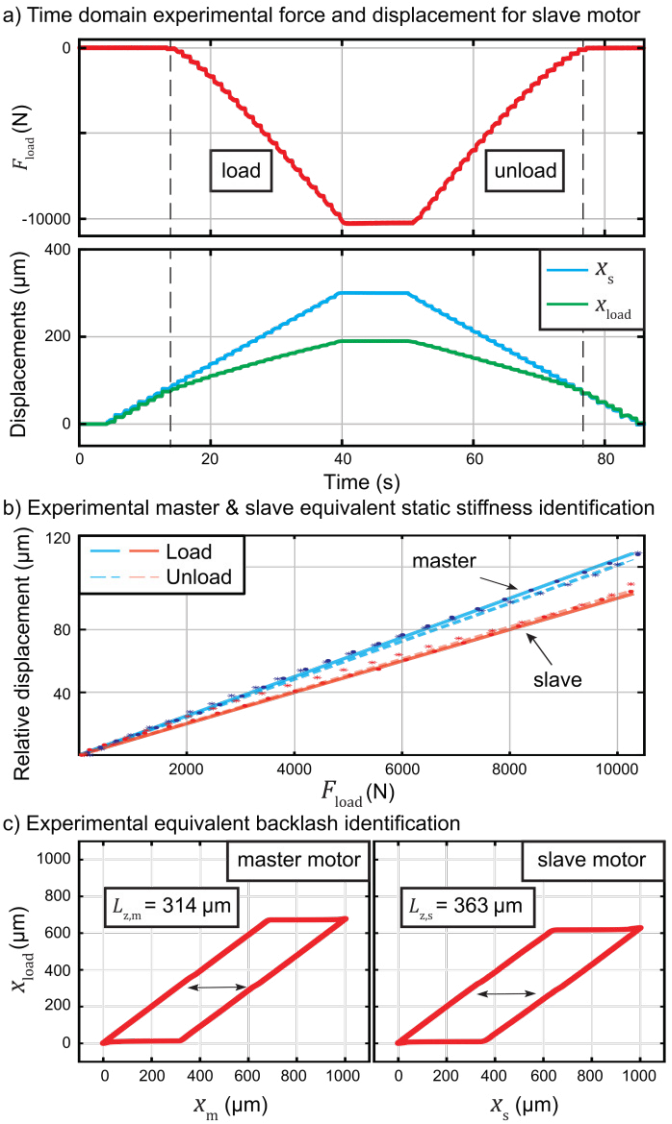

Fig. 4. *Experimental identification of double pinion and rack feed drive model parameters.*

4. Model validation

At the same location where the identification has been conducted, the machine control is returned to the original master-slave coupling configuration as shown in Fig. 1.a. With the machine load movement constrained, a CNC position command of 300 µm is commanded, resulting in approximately 20kN of F_{load}. Fig. 5.a compares the experimental and simulated results of a static stiffness test. Fig. 5.a shows the displacements (x_{load}, x_s and x_m) during the loading and unloading stages. The load displacement closely matches the commanded value since the position loop is closed with this signal. However, this is not the case for the displacements of the motors. For the slave motor, the displacement reaches about 400 µm at maximum load, aligning with the simulated result. In contrast, the master motor displacement is significantly larger and shows a sharp jump when the rack and pinion contacts change from configuration ② to ③ in Fig.2. The load force required for this configuration change depends on the commanded preload level. This effect can be explained by Fig. 5.b, which shows the torque of each motor over time during the test. At a certain point, F_{load} becomes large enough to counteract the commanded preload torque, causing the torque in one motor to drop to zero, and the electronic preload is lost. As the force continues to increase, the pinion rotates and engages with a different flank of the rack, depending on the load direction. This transition between configurations (② with ① or ③) causes the master motor encoder to detect more displacement than the slave motor encoder, as shown in Fig. 5.a. This change in polarity is also reflected in the measured torques (Fig. 5.b).

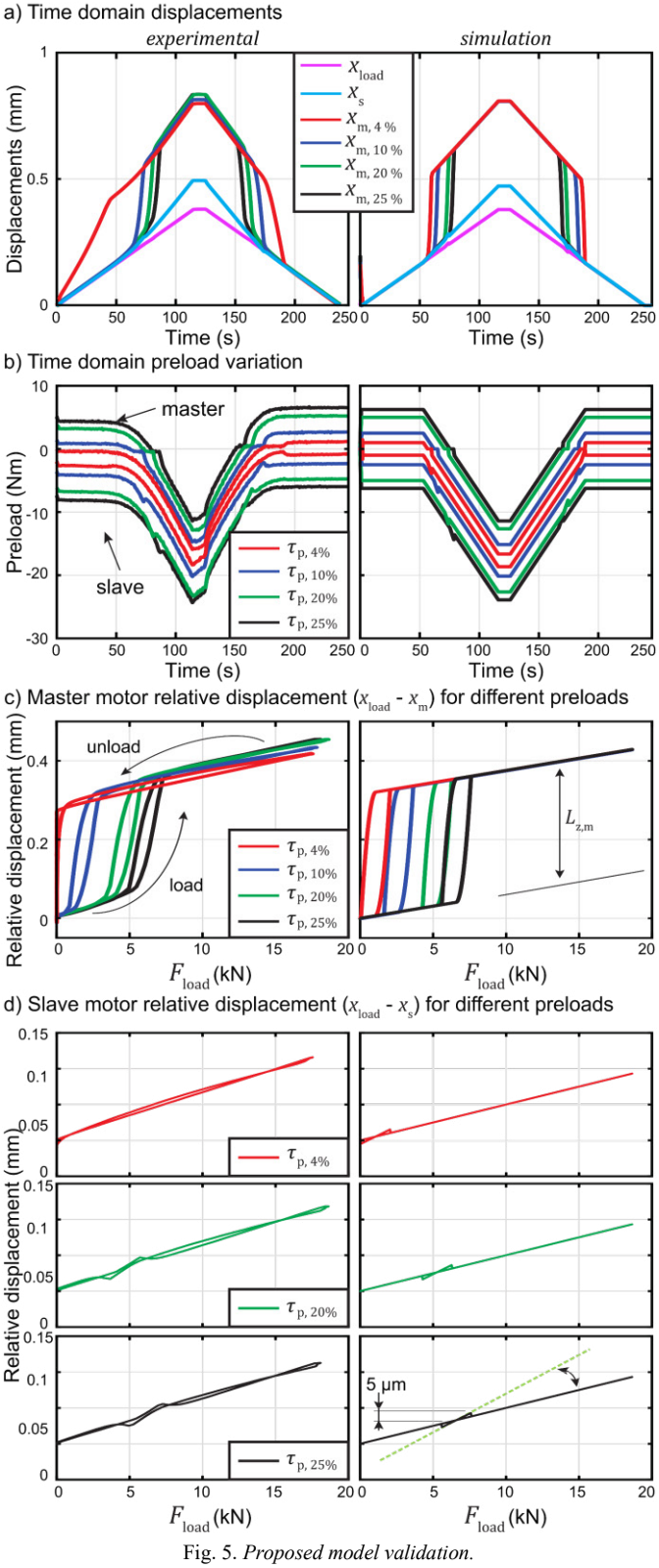

Fig. 5. *Proposed model validation.*

Four different preload levels ($\tau_p = 4$, 10, 20 and 25 %) have been tested to analyze this effect. Both experimental and simulated results show that the point at which preload is lost varies with the commanded preload level. Fig. 5.c illustrates the relative displacement of the master motor for these preload levels, based on data from Fig. 5.a. A significant increase in the force level causing pinion contact loss is observed between the 4% preload and the higher levels, ranging from 1100 N to 5300 N or 6600 N. As the load increases, the pinion teeth re-engage, and linear behavior is restored until the maximum tested force is reached. There is a noticeable reciprocity between the load and unload stages. The relative displacement between the points of contact loss and recovery is determined by the backlash value (Fig. 5.c).

As a coupled system, the slave motor is also affected by preload loss, showing a 5 µm change in relative displacement (Fig. 5.d). This indicates that when preload is lost, the entire F_{load} is transmitted through the slave motor, reducing stiffness and causing the observed over-displacement.

4.1. Equivalent stiffness variation analysis

From the relative displacements shown in Fig. 5.c&d, the equivalent stiffness variation is calculated using Eq. 5 (applicable to both k_m and k_s). It is assumed that F_{load} is evenly distributed between the two motors under full contact conditions. However, the pinion-rack contact condition (k_{p-r}) during characterization can affect the calculated stiffness values (k_m and k_s). According to the DIN ISO 6336 standard, the equivalent mesh stiffness is influenced by the teeth in mesh and contact ratio. To analyze variability caused by contact ratio changes, two bounds have been established.

$$k_{m,s} = \frac{\Delta F_{Load}}{\Delta \delta_{m,s}} = \frac{0.5\left(F_{Load}(t+1) - F_{Load}(t)\right)}{\delta_{m,s}(t+1) - \delta_{m,s}(t)} \quad (5)$$

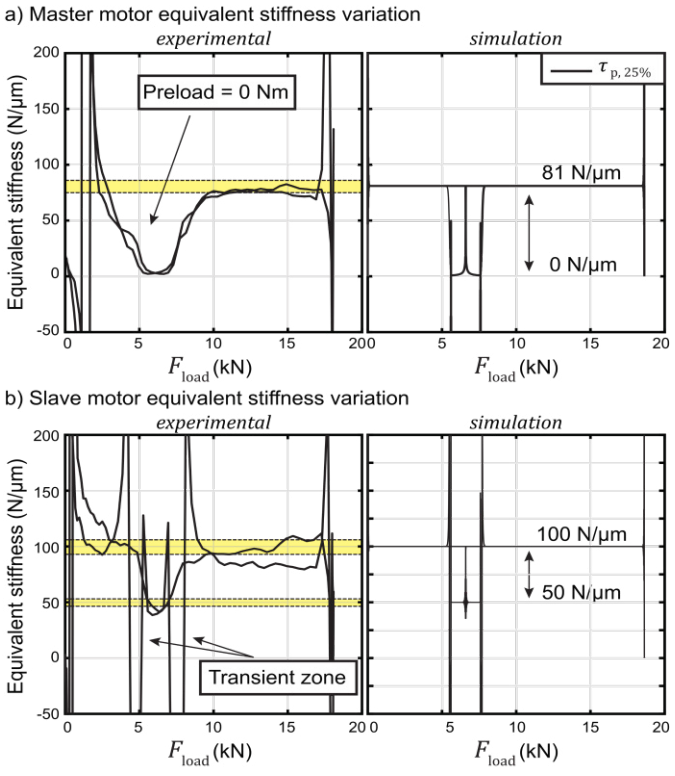

Fig. 6. *a) Master; b) Slave motor static stiffness variations.*

The lower bound assumes a single pair of teeth in mesh, while the upper bound considers two pairs, resulting in equivalent mesh stiffnesses ranging from 550 to 962 N/µm. Adding these bounds to the total equivalent stiffness (Eq. 2) shows a variation of 7.4% for the master motor and 9.5% for the slave, as shaded in Fig. 6.a&b. Fig. 6.a shows the master motor's stiffness variation under a 25% preload. As F_{load} increases, the stiffness initially drops to 0 N/µm but eventually converges to 81 N/µm. The unload phase follows a similar trend. The simulated behavior aligns with experimental results. For the slave motor at a 25% preload (Fig. 6.b), initial stiffness is around 100 N/µm. Due to contact loss in the master motor, stiffness drops by half as the slave motor alone bears the full load. When contact is regained, a high stiffness transient zone occurs before converging back to approximately 100 N/µm. Torque distribution between master and slave motors varies (Fig. 5.b), impacting preload loss force predictions when one motor's torque reaches zero. Although experimental backlash may differ slightly from the dead zone model, the proposed rack and pinion feed drive system accurately reflects experimental findings.

4.2. Static stiffness analysis at the machine ram

The identified effect occurs not only when force is applied at the column but also near the cutting point, such as the machine ram. To prevent damage, the maximum load force has been reduced to 10 kN. Fig. 7 shows various experimental measurements of relative displacements. For the master and slave motors, relative displacement is calculated between each motor's encoder and the linear encoder. For the ram, it is calculated between the linear encoder and the displacement measured by an inductive sensor (IWRM 04U9701). The ram tip stiffness is relatively linear with force level and is unaffected by the rack and pinion preload.

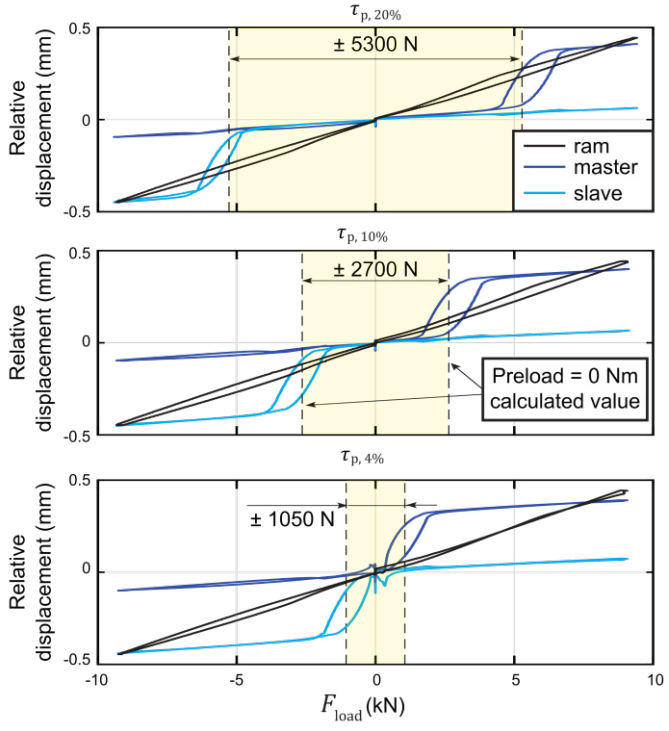

Fig. 7. *Experimental ram, master and slave motors static stiffness response.*

Since the position loop is closed with the linear encoder, the backlash effect is minimized and mainly appears at the feed drive level. However, axis clearance affects the linearity of the feed drive mechanism and may increase tracking or following errors. By considering the commissioned preload level and the linear-rotary conversion factor (Ktr), the expected load force at which preload is lost can be identified. Within the identified bounds, preload presence ensures linearity. The three cases analyzed show a similar pattern, with differences primarily at the preload loss point, ranging from ±1050 N to ±5300 N.

5. Conclusions

This paper analyzed the influence of commanded preload amplitude on the static stiffness of an electronically preloaded double pinion and rack feed drive system. The research shows that the transition of the pinion flank due to existing backlash, resulting from a static disturbance, cannot be ignored. Specifically, variations in the commanded preload level influence both the machine's acceleration capabilities and the nonlinear behavior of the stiffness. The proposed model effectively predicts the experimental trends, indicating that increasing electronic preload does not result in higher stiffness values for either the master or slave motors. For instance, at a preload of 25%, the identified stiffness for the master motor varies from 0 N/µm to approximately 81 N/µm, while for the slave motor, it ranges from 100 N/µm to half of that value during contact loss.

Even though backlash-induced nonlinearity is limited near the cutting point (i.e. the machine tool ram), there are other major concerns that should be addressed. First, having one of the two pinions disengaged increases operational and control uncertainty. It also modifies the feed drive system equivalent stiffness up to 50% (as indicated in Fig. 6), as the entire force is transmitted through a single contact point. Secondly, speed or rate at which this contact loss occurs is crucial, as it can act as an excitation source, potentially inducing vibratory behavior. Additionally, in heavy-duty roughing operations, the combined static and dynamic cutting forces can create perturbations at the machine feed drive level. When these perturbations interact with the contact loss uncertainty, stiffness variations and feed drive controller effect, they can lead to undesirable effects. To mitigate these issues, maintaining a relatively high preload value (such as 20%, where the contact loss begins at 5300N) can help in reducing the occurrence of such problems by granting feed drive stiffness linearity.

Further work will deal with the integration of machine tool Finite Element model dynamics with the feed drive model and the addition of complete nonlinear mesh stiffness characteristics.

Acknowledgements

This research was funded by the Basque Country Business Development Agency (SPRI) under the ELKARTEK 2024 MECACOGNIT (KK-2024/00030) project.

References

[1] Altintas, Y., Verl, A., Brecher, C., Uriarte, L., and Pritschow, G. Machine tool feed drives. CIRP annals, 2011, 60(2), 779-796.
[2] Pritschow, G., A comparison of linear and conventional electromechanical dives. CIRP annals, 1998, 47.2: 541-548.
[3] De Lacalle, N. L., and Lamikiz, A., Machine tools for high performance machining, Springer Science & Business Media, 2008.
[4] Uriarte, L., Zatarain, M., Axinte, D., Yagüe-Fabra, J., Ihlenfeldt, S., Eguia, J., and Olarra, A. Machine tools for large parts. CIRP annals, 2013, 62(2), 731-750.
[5] Oyanguren, A., Zahn, P., Alberdi, A. H., Larrañaga, J., Lechler, A., & Ulacia, I. (2016). Preload variation due to temperature increase in double nut ball screws. Production Engineering, 10, 529-537.
[6] Oyanguren, A., Larranaga, J., & Ulacia, I. (2018). Thermo-mechanical modelling of ball screw preload force variation in different working conditions. The International Journal of Advanced Manufacturing Technology, 97, 723-739.
[7] Frey, S., Walther, M., and Verl, A., Periodic variation of preloading in ball screws. Production Engineering, 2010, 4(2-3), 261-267.
[8] Verl, A., Frey, S., and Heinze, T., Double nut ball screw with improved operating characteristics. CIRP Annals, 2014, 63(1), 361-364.
[9] N. N., 1989, ISO 3408-3:2006 Acceptance conditions and acceptance test.
[10] Verl, A., and Frey, S., Correlation between feed velocity and preloading in ball screw drives. CIRP annals, 2010, 59(1), 429-432.
[11] Zhou, C. G., Feng, H. T., Chen, Z. T., and Ou, Y., Correlation between preload and no-load drag torque of ball screws. International Journal of Machine Tools and Manufacture, 2016, 102, 35-40.
[12] Deutsches Institut für Normung, 1978, DIN 3967:1978 Tooth allowances, tooth thickness tolerances system of gear fits principles: Backlash.
[13] Lloyd W.B., and Staehlin, J.H., Anti-backlash gear assembly, U.S. Patent No. 4,072,064, Washington, DC: U.S. Patent and Trademark Office, 1978.
[14] Hale, L. C., and Slocum, A. H., Design of anti-backlash transmissions for precision position control systems. Precision engineering, 1994, 16(4), 244-258.
[15] O'neill Robert F., Anti-backlash gears, U.S. Patent No. 3,127,784. Washington, DC: U.S. Patent and Trademark Office, 1963.
[16] Prodan, D., Petre, M., Constantin, G., and Bucuresteanu, A., Eliminating the backlash of circular feed drives of cnc vertical lathes. Proceedings in Manufacturing Systems, 2016, 11(1), 27.
[17] "REDEX: Rack and Pinions." [Online]. Available: www.redex-andantex.com (accessed on 23 May 2024).
[18] Zirn, O., Machine tool analysis: modelling, simulation and control of machine tool manipulators, A habilitation thesis, ETH Zurich, 2008, Zurich, Switzerland.
[19] Engelberth, T., Apprich, S., Friedrich, J., Coupek, D., and Lechler, A., Properties of electrically preloaded rack-and-pinion drives. Production Engineering, 2015, 9(2), 269-276.
[20] Verl, A., Leipe, V., Dual motor position feedback control for electrically preloaded rack and pinion drive systems to increase accuracy. CIRP Annals, 2024, 73(1);313-316.
[21] Heidenhain, "Technical Manual TNC640," 2015.
[22] Verl, A., and Engelberth, T., Adaptive preloading for rack-and-pinion drive systems. CIRP Annals, 2018, 67(1), 369-372.
[23] Franco, O., Beudaert, X., and Erkorkmaz, K., Effect of Rack and Pinion Feed Drive Control Parameters on Machine Tool Dynamics. Journal of Manufacturing and Materials Processing, 2020, 4(2), 33.
[24] Cooley, C. G., Parker, R. G., A review of planetary and epicyclic gear dynamics and vibrations research. Applied Mechanics Reviews, 2014, 66(4).
[25] Ulacia, I., Sánchez, M. B., Iñurritegui, A., Arana, A., Larrañaga, J., and Pedrero, J. I., Theoretical analysis of transmission error in rack and pinion systems, MATEC Web of Conferences (Vol. 387, p. 01001). EDP Sciences.
[26] Moradi, H., and Salarieh, H., Analysis of nonlinear oscillations in spur gear pairs with approximated modelling of backlash nonlinearity. Mechanism and Machine Theory, 2012, 51, 14-31.
[27] Margielewicz, J., Gąska, D., and Litak, G., Modelling of the gear backlash. Nonlinear Dynamics, 2019, 97(1), 355-368.